

# Spectrophotometer analysis of Holocene sediments from an anoxic fjord: Saanich Inlet, British Columbia, Canada

Maxime Debret <sup>a,\*</sup>, Marc Desmet <sup>a,1</sup>, William Balsam <sup>b</sup>, Yoann Copard <sup>c</sup>,  
Pierre Francus <sup>d</sup>, Carlo Laj <sup>e</sup>

<sup>a</sup> EDYTEM Laboratory, UMR 5204, University of Savoie, CISM, Campus Scientifique, F-73376 Le Bourget du Lac Cedex, France

<sup>b</sup> Department of Geology, University of Texas at Arlington, Arlington, TX 76019, USA

<sup>c</sup> UMR 6143 M2C, Department of Geology, University of Rouen, 76131 Mont-Saint Aignan Cedex, France

<sup>d</sup> Institut National de la Recherche Scientifique (INRS), Centre Eau, Terre et Environnement, rue de la Couronne, Québec, (Québec) Canada, G1K 9A9

<sup>e</sup> Laboratoire des Sciences du Climat et de l'Environnement (LSCE), Unité Mixte CEA-CNRS, Avenue de la Terrasse, 91198 Gif-sur-Yvette Cedex, France

Received 15 November 2004; received in revised form 21 December 2005; accepted 23 January 2006

## Abstract

A borehole core through the Holocene sediments of Saanich Inlet (British Columbia, Canada) was analyzed using high-resolution spectrophotometry to determine whether spectral–signal variations can be used as environmental/climatic proxies. The effects of post-drilling oxidation and water loss on the core sample were assessed by comparing spectral measurements taken onboard the research ship immediately after the core was opened with shore-based measurements taken one year later. For Saanich Inlet sediments, the shore-based measurements provided more reliable indications of the degree of basin anoxia. Our spectral analyses allowed us to identify all the major features of the Saanich Inlet sediment sequence (Mazama ash and Fraser River Drainage stratigraphic markers, oxygenation state of the basin). By using the first derivative value at 675 nm as a proxy for changes in organic matter content and the colorimetric parameter  $b^*$  as an indicator of diatom content, we were able to recognize changes in terrestrially derived organic matter (OM) and diatom concentrations in the sediment. We suggest that these variations are due to changes in upwelling intensity and fluctuations in sea level during the Holocene. Our results confirm the potential value of spectrophotometry in identifying sediment composition and in reconstructing paleoenvironments.

© 2006 Elsevier B.V. All rights reserved.

**Keywords:** spectrophotometry; reflectance; Holocene; Saanich Inlet; British Columbia; organic matter; diatoms; CIE  $L^*a^*b^*$ ; upwelling

## 1. Introduction

It is standard practice onboard a research vessel for cores to be subject to visual description and a series of preliminary measurements, typically including magnetic susceptibility, GRAPE (Gamma Ray Attenuation Porosity Evaluator), P-wave velocity and video capture.

\* Corresponding author. Laboratoire de Glaciologie et de Géohydrologie de l'Environnement (LGGE) CNRS BP 96, F-38402 St. Martin d'Hères Cedex, France. Tel.: +33 4 76 82 42 44; fax: +33 4 76 82 42 01.

E-mail address: debret@lgge.obs.ujf-grenoble.fr (M. Debret).

<sup>1</sup> Laboratoire des Sciences de l'Environnement, ENTPE, Rue Maurice Audin, 69518 Vaulx en Velin, France.

During a number of recent oceanographic cruises, researchers have analyzed a new sediment property, spectral reflectance (Mix et al., 1992; Balsam et al., 1997), which allows the visual properties of sediments to be quantified. Although a number of studies have been performed on oxic sediments, this technique has rarely been applied to anoxic sediments. In this study, the data provided by reflectance spectrophotometry analyses of sediment samples from Saanich Inlet was used to identify the components of the sediment and to draw up paleoenvironmental reconstructions.

Saanich Inlet is a temperate fjord on the southeastern side of Vancouver Island, British Columbia (B.C.). Sedimentation rates are high and, as the basin is anoxic, the resulting deposits are little affected by bioturbation, allowing fine temporal resolution. The main characteristics of the basin, including seismic stratigraphy (Mosher and Moran, 2001) and paleo-seismicity (Blais-Stevens and Clague, 2001), have been defined from detailed analyses of cores ODP 1033 and 1034. Paleoenvironmental studies have been carried out using a variety of markers, such as diatoms (McQuoid and Hobson, 2001), fish (O'Connell and Tunnicliffe, 2001; Tunnicliffe et al., 2001), pollen (Pellatt et al., 2001), and geochemical analyses, which have provided information on the origin of organic matter (OM) (McQuoid et al., 2001; Whiticar and Elvert, 2001; Calvert et al., 2001; Timothy et al., 2003). However, very few studies have examined differences in sediment color. Nederbragt and Thurow's (2001) use of digital color analysis to measure varve thickness and thereby infer deposition rates in Saanich Inlet sediments is a notable exception.

In this paper, we further explore the use of spectrophotometric data to evaluate and identify sediment components and we investigate the use of reflectance spectrophotometry as a high-resolution tool for tracking environmental changes and distinguishing variations in the origin of sediment in the basin. Our work was based on analyses of core MD02-2490, drilled by the *RV Marion Dufresne* during the Mona study cruise along the western margins of North America, which was undertaken as part of the IMAGES VIII (International Marine Past Global Changes Study) program.

## 2. Study site

### 2.1. Saanich Inlet and the MD02-2490 core

Saanich Inlet (Fig. 1) is a temperate fjord on the southeastern side of Vancouver Island, British Columbia (B.C.). It is 24 km long, between 0.4 and 7.6 km wide and has a maximum depth of 234 m (Herlinveau, 1962).

The mouth of the basin is partially blocked by a 75 m-deep sill, formed by a moraine. This sill prevents most deep-water circulation (Carter, 1934; Herlinveau, 1962), but it does allow nutrients and sediments to enter the basin from the Cowichan River to the north. The Cowichan River is the largest single source of sediment to Saanich Inlet, transporting clay-rich material into the inlet via Satellite Channel during the autumn/winter discharge (Herlinveau, 1962). The only river that flows directly into Saanich Inlet is the Goldstream River, but it only supplies a small percentage of the 90,000 tons of sediment deposited each year (Gross et al., 1963).

The anoxic conditions that characterize the inlet are the result of several factors, including weak circulation in the inlet, the presence of the sill, strong primary productivity and the restricted input of new water to the basin. A second halocline, below sill depth, marks the upper boundary of an almost permanently anoxic zone in which there is no benthic fauna and, therefore, no bioturbation. This allows the preservation of annual varve-like laminae (Gross et al., 1963; Sancetta and Calvert, 1988; Bobrowsky and Clague, 1990; Blais, 1995), composed of two distinct sediment types: a "silt and clay" layer, deposited during fall and winter, and a light-colored, diatom-rich layer that forms during major spring and summer blooms. Sometimes a third, gray "clay" lamina, can be distinguished. It is interpreted as the result of flood events from the Cowichan River (Blais-Stevens and Bornhold, 1998). Varve thickness varies from 1 mm to more than 1 cm.

Sedimentation rates for organic matter are uniform throughout the basin, but the concentration of organic matter is dependent on the degree to which it is diluted by terrigenous sediments from the Cowichan River: sediments in the southern part of the basin have lower organic matter concentrations than sediments in the northern part.

We analyzed sediment core MD02-2490 (048°35.37' N, 123°30.17' W), which was drilled in the narrowest part of the inlet (~2 km-wide) at a water depth of 224 m. The sediments of the 51.07 m-long core represent the entire Holocene and terminate in a Late Pleistocene sand layer. MD02-2490 was drilled close to the site of ODP 1033 (048°35.438' N, 123°30.201' W), Leg 169S, allowing comparisons to be made between the two cores.

### 2.2. Physiographic and geologic history

The oldest glaciogenic deposits in ODP 1033 and 1034 have been dated ( $^{14}\text{C}$ ) at  $13,270 \pm 60$  yr BP (Cowan, 2001), suggesting the deglaciation of the study area probably occurred around 14,000 yr cal. BP. However, at this time, the peninsula that would contain

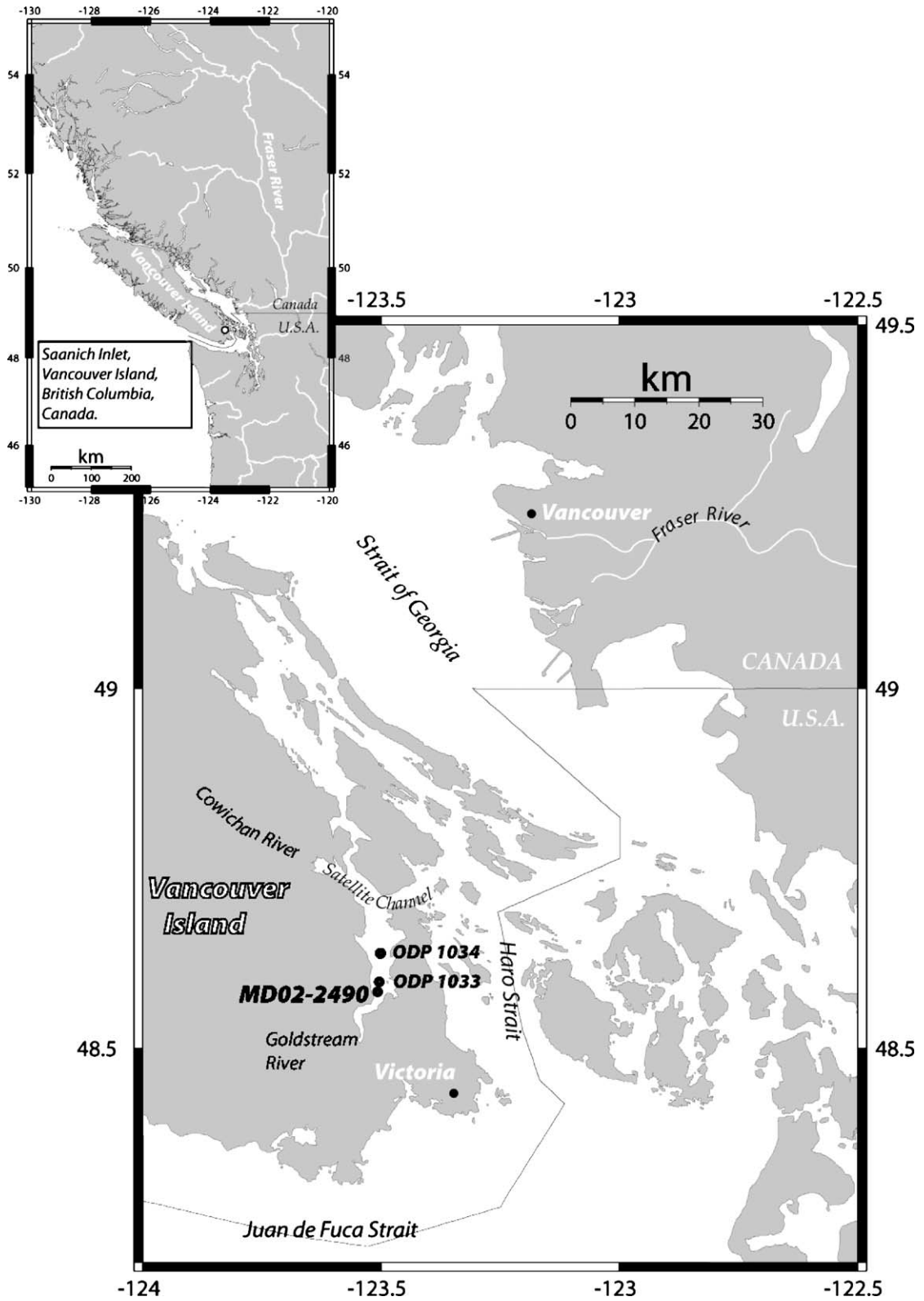


Fig. 1. Location map showing Saanich Inlet on Vancouver Island, British Columbia and the location of ODP Holes 1033 and 1034 (Leg 169S) and core MD02-2490 (Mona cruise).

Saanich Inlet had not yet completely emerged. With the progressive deglaciation of the southern part of Vancouver Island, from 12,000–10,000 yr cal. BP, melt water input and sediment supply to the basin decreased (Huntley et al., 2001). Around 11,000 years ago, the draining of a pro-glacial lake on the Fraser River led to the deposition of a bed rich in “exotic” material in Saanich Inlet (Blais-Stevens et al., 2003). The record of core MD02-2490 begins around this period. By 10,873–10,636 yr cal. BP the glaciers in the Coast Mountains were in similar positions to where they are now (Clague and James, 2002). Paleo-drainage channels, 10 m below current sea level and dated at between 8000 and 9000 yr cal. BP, are interpreted as indicating a lower sea level (Huntley et al., 2001). As changes in sea level can significantly modify coastal geography, Huntley et al. (2001) have suggested that the rise in sea level in Saanich Inlet had an impact on the basin’s oceanography. During the Middle Holocene (4000–8000 yr cal. BP), sea level started rising, to reach its present level around 4000 yr cal. BP. The watershed and oceanography of the study area then stabilized (Huntley et al., 2001).

### 3. Methods

#### 3.1. Shipboard measurements

Spectral analysis of the core was carried out onboard the *Marion Dufresne* using a Minolta CM-2002 spectrophotometer. Measurements were taken at 20 nm increments over the range 400 to 700 nm. The downcore interval was 5 cm. These analyses were done about 0.5 h after the core was opened. Upon opening, the core was covered with polyethylene film to prevent water loss, to minimize color changes due to oxidation (Chapman and Shackleton, 1998) and to avoid any contamination from the spectrophotometer. The effects on the core of water loss and/or oxidation during the 30 min that lapsed between core opening and spectral analysis can be considered negligible. Spectral measurements were taken directly on the core surface through the polyethylene film; however, care was taken to use a polyethylene film with physical and optical properties that would not bias the color ( $a^*$ ,  $b^*$ ) and brightness ( $L^*$ ) measurements.

#### 3.2. Shore-based measurements

Sediment color analyses were carried out at the Laboratory EDYTEM using a Minolta CM 2600d, which provides reflectance intensity measurements for visible wavelengths between 400 and 700 nm. Measure-

ments were taken at 10 nm intervals. We used the Specular Component Excluded–CIE  $L^*a^*b^*$  mode (Minolta CM-2002 handbook) in order to eliminate any bias due to specular reflection. The  $L^*a^*b^*$  mode covers the whole spectrum perceived by the human eye; it is independent of any color reproduction technology, and therefore of any peripheral apparatus. It includes the mode colors RGB and CMYK. Analyses were carried out using a D65 illuminant (Minolta CM-2002 handbook), which corresponds to average daylight, with a color temperature of 6504 K, and an 8 mm aperture. Measurements were taken at 1 cm intervals along the entire length of the core, thereby providing an almost continuous record of sediment changes. Because we only had access to U-channel samples, and because the U-channel support was too thick to allow direct measurements to be taken, our analyses were carried out on 5 mm-thick slices cut from the samples. These spectral measurements were taken in the summer of 2003, one year after the shipboard measurements taken on the *Marion Dufresne*. Although Chapman and Shackleton (1998) recommended calibrating the instrument with respect to a white standard covered with polyethylene film, we decided to calibrate the spectrophotometer without the polyethylene film because the instrument is set up to identify specific reflectance values stored in its internal memory (Balsam et al., 1997). Calibration was performed using a white calibration tile referenced to an international  $\text{BaSO}_4$  standard. The instrument was re-calibrated at the beginning of each 1.50 m section of U-channel.

Low-field magnetic susceptibility ( $\kappa$ ) was measured in a magnetically quiet laboratory using U-Channels and a small diameter Bartington coil, which allows a resolution of 4 cm — very similar to the resolution obtained using a cryogenic magnetometer.

#### 3.3. Data processing

Raw values of  $b^*$  were seen to be highly variable. In order to investigate this high frequency variability in the color signal, we removed larger-scale trends using the difference of the sum of the squares of the variations subtracted from a 5-point moving average.

First derivative methods were applied because the studies of Barranco et al. (1989), Deaton and Balsam (1991), Balsam and Deaton (1991, 1996), Balsam et al. (1998), Herbert et al. (1992), and Mix et al. (1992) have shown that some components of marine sediments exhibit distinct spectral signatures. According to these researchers, first derivative peaks and slope breaks between 400 and 700 nm are indicative of specific

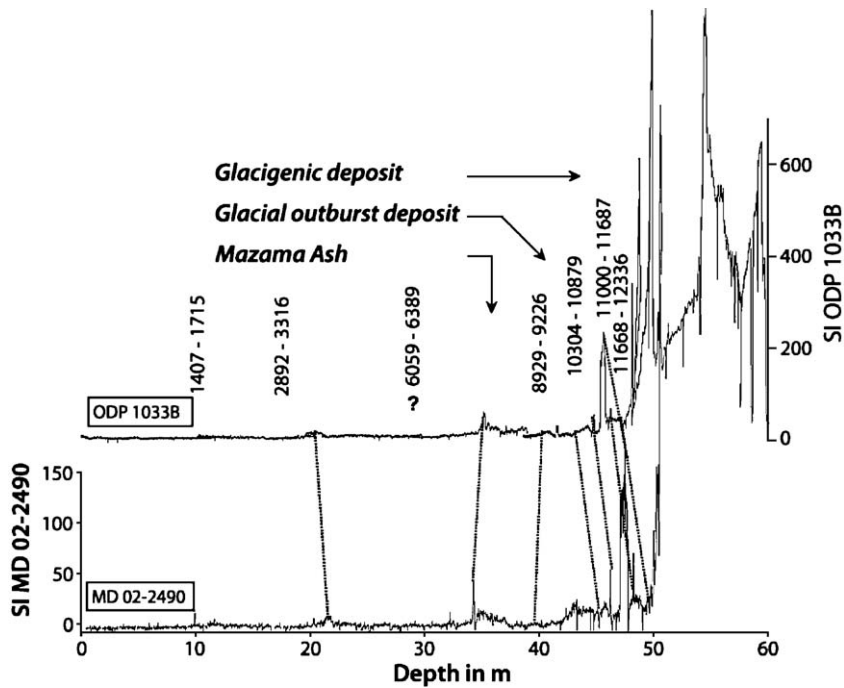


Fig. 2. Comparison of magnetic susceptibility (MS) from ODP 1033B and MD02-2490. Magnetic susceptibility in SI has been reported on the Y axis. Ages ( $^{14}\text{C}$  cal. BP) referred in *Initial Reports Proceedings of the Ocean Drilling Program* permit the establishment of an age model by matching the magnetic susceptibility of both records. The ODP radiocarbon ages identified on MS are reported on the MD02-2490 signal.

sediment components such as iron oxide minerals (555, 565, 575 nm); the oxyhydroxide goethite (445 and 525 nm); the clay minerals illite, montmorillonite and chlorite; calcite and organic components of the sediment

(from 605 to 695 nm) (Deaton and Balsam, 1991; Balsam et al., 1998; Balsam and Beeson, 2003). Here we investigate the possibility of using the first derivative of the visible spectrum (percentage reflectance per

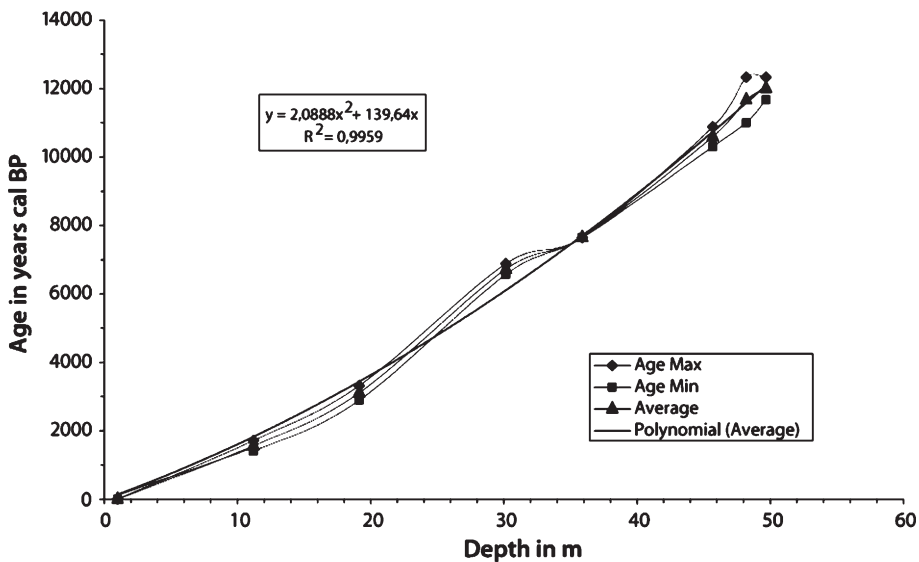


Fig. 3. Age model. Age (cal. BP) referred to in *Initial Reports Proceedings of the Ocean Drilling Program* are expressed with minimum and maximum age after correction for the reservoir effect. The polynomial curve used to obtain age vs. depth was established with the average age and shows a good  $R^2$  (0.9959). The Mazama ash layer (3589 cm, 7645 yr cal. BP) is the best marker to validate the age model.



nanometer) to investigate the sedimentological components of core MD02-2490.

#### 4. Age model

Unless stated otherwise, all the ages given in this article are calendar ages.

Two well-dated stratigraphic markers were identified in the MD02-2490 core: the Mazama ash and a silty-clay horizon produced by the catastrophic drainage of a pro-glacial lake in the Fraser River Valley. The Mazama ash, which was produced by the cataclysmic eruption of Mount Mazama in Oregon (USA), occurs at a core depth of 3589 cm and has been dated at 7645 yr BP (Bacon, 1983 reconfirmed in Blais-Stevens et al., 2001). In Saanich Inlet, more than 700 km from the volcano, the compacted ash forms a 1 cm-thick layer (Blais-Stevens et al., 2001 give the thickness of this horizon as 2 cm). The second stratigraphic marker consists of a gray, illite and muscovite-rich silty-clay that was derived from the Pleistocene sediments of the Fraser River Valley (Blais-Stevens et al., 2003). It occurs at a depth of 4709 cm and has been dated at around 11,000 yr BP (Blais-Stevens et al., 2003). The contact between this clay horizon and the olive-colored sediments below is very sharp.

In addition to the stratigraphic markers, our age model is based on the correlation of magnetic susceptibility (MS) data between core MD02-2490 and ODP Hole 1033. This correlation also allows us to extrapolate the  $^{14}\text{C}$  chronology established for ODP 1033 to MD02-2490, thereby providing a precise age

framework for our downcore MS peaks (Fig. 2). The age model was drawn up by assigning minimum and maximum dates to the stratigraphic levels used for correlation, because maximum and minimum ages were given for the ODP horizons. The age model was then based on a polynomial equation derived from the average ages of the ODP horizons (Fig. 3).

We applied a reservoir age of  $801 \pm 23$  yr, measured using marine shells (Robinson and Thompson, 1981). This is consistent with the reservoir age of  $798 \pm 50$  yr calculated to ODP 1033 (Bornhold et al., 1996). More recently, Blais-Stevens confirmed this reservoir age using ODP wood/shell pairs. Hutchinson et al. (2004) demonstrated that the reservoir age for ODP 1033 could vary between  $670 (\pm 80)$  and  $950 (\pm 80)$  yr. The quality of our age model was evaluated with respect to the Mazama ash, which has been dated at 7645 yr BP. The 57-yr difference between the  $^{14}\text{C}$  age and the age model (7702 yr BP) is within the margin of error for the  $^{14}\text{C}$  data as estimated by Hutchinson et al. (2004).

#### 5. Results

##### 5.1. Data processing

The  $L^*$  (lightness or luminance) and  $a^*$  (red/green variation) curves were difficult to interpret. For  $L^*$  this difficulty may be due to the presence of illite and to the anoxic conditions. White/black variations are classically interpreted as being due to variations in carbonate content (Schneider et al., 1995; Balsam et al., 1999), however such an interpretation could not be applied here

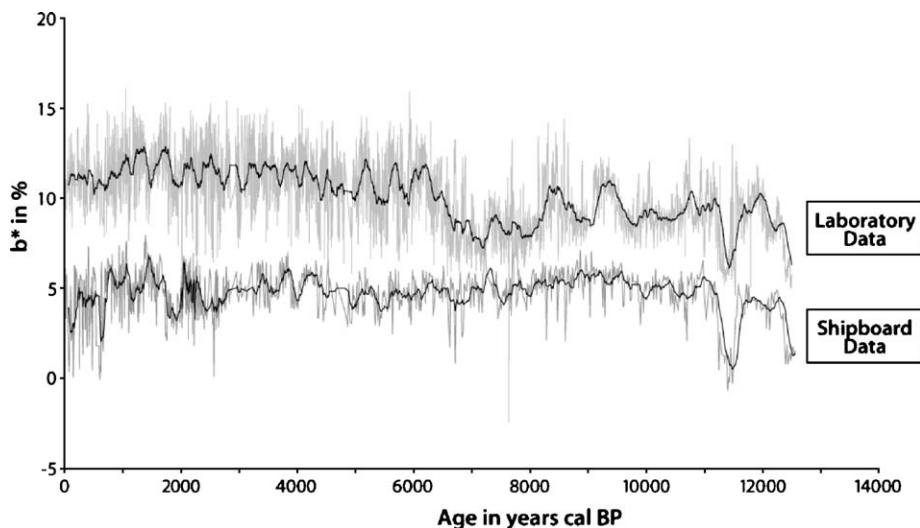


Fig. 4. Comparison between  $b^*$  taken on board the *Marion Dufresne* and  $b^*$  from our laboratory-based instrument.

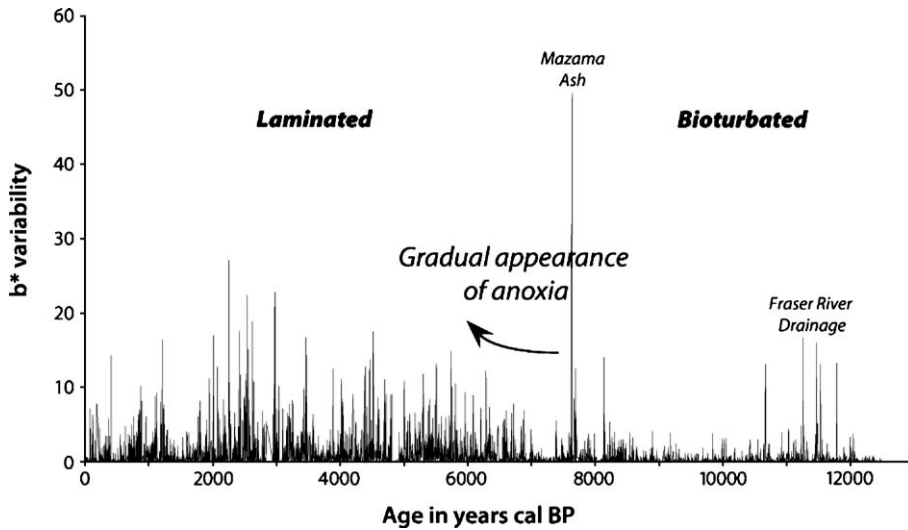


Fig. 5. The variability of  $b^*$  showing the two major states of the Saanich Inlet basin. In order to investigate short term variability of the color signal, we also removed the trend using the difference of the sum of squares of the variations subtracted from a 5-point moving average. A low variability implies bioturbated sediment and oxic conditions whereas a high variability characterizes laminated sediments. The transition between laminated and non-laminated sediments occurs around 7000 yr BP (southern part of the fjord). The two stratigraphic markers explain high variability during the bioturbated period. Indeed a sharp difference of color between Mazama Ash (white), for example and sediment (olive) implies a high variability.

for two reasons. Firstly, the water is very acidic, due to the intense primary productivity and anoxic conditions, which results in high carbonate dissolution rates (Timothy et al., 2003). Secondly, Saanich Inlet sediments are composed primarily of white clay, which interferes with the measurement of  $L^*$ . Balsam et al. (1999) showed that the non-carbonate fraction of the sediment has a major influence on  $L^*$ . If this fraction is dominated by white minerals, such as kaolinite, the reflectance of  $L^*$  will show only a slight change as carbonate content increases. Conversely, dark minerals

such as illite can substantially lower  $L^*$  (Balsam et al., 1999).

Similarly, the CIELab values of  $a^*$  (used by Helmke et al. (2002) as an ice rafted debris marker) ranged from  $-2$  to  $+2$ . The Minolta handbook describes this range as achromatic and its interpretation is complex.

Unlike the first two parameters, significant changes (from 5% to 20%) were observed in the reflectance values for  $b^*$  (blue/yellow variation). Smear slides of sediment showed that the light-colored laminae are diatom-rich (consisting of alternating layers of diatom

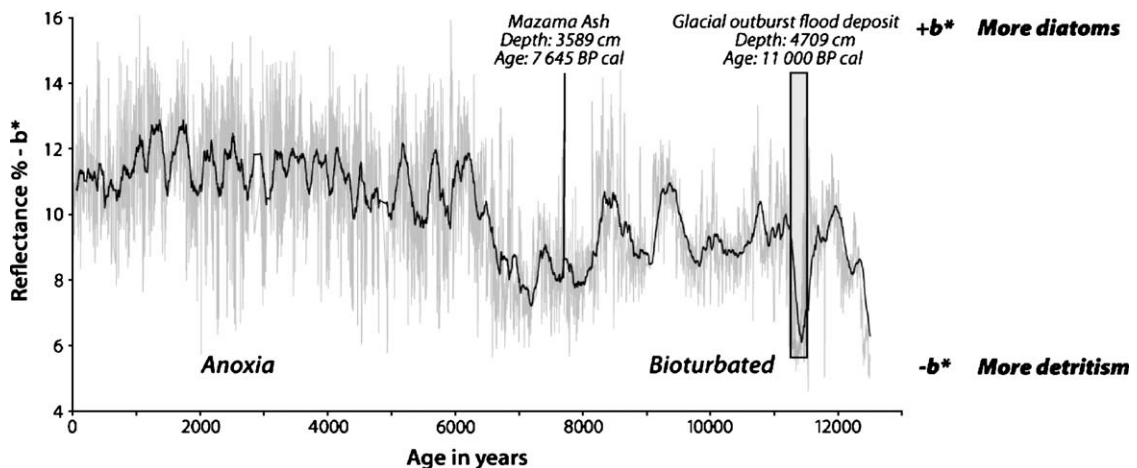


Fig. 6.  $b^*$  variations during the Holocene. Also shown are the two stratigraphic markers, the Mazama ash and Fraser River drainage. The thick line has been calculated by a 45-point moving average.

ooze and diatomaceous mud deposited in the spring, summer and fall). These laminae, which tend towards yellow (high  $b^*$  values), alternate with darker laminae (low  $b^*$  values) rich in detrital material (olive to olive-gray silty-clays deposited during the winter). Thus, changes in the value of  $b^*$  can be used to differentiate between these two major sediment types.

### 5.2. Shore-based vs. land-based measurements

We compared the measurements to evaluate color changes between the first series of measurements made 30 min after the core was opened (largely unoxidized) and later measurements (fully oxidized). 30 min is about the shortest time that could be guaranteed for all samples to insure that we are looking at the same degree of oxidation in every sample.

The laboratory spectra tended more towards the yellow than the onboard measurements. The  $b^*$  signals recorded onboard and in the laboratory were also very different. The onboard measurements showed only a slight variability, except for the last 4000 yr BP, where the signal was very irregular. The laboratory measurements showed an apparent cyclicity, which was less pronounced at the bottom of the core, but clearly distinguishable from the recorded noise. However, this cyclicity was different on either side of a transition phase marked by a distinct increase in  $b^*$  from  $<10\%$  to  $>10\%$  (Fig. 4). The two stratigraphic markers can be distinguished in both sets of measurements. The white color and low  $b^*$  values (7.5%) recorded for the 7645 yr BP Mazama ash layer contrast with the background sedimentation. On each side of this ash deposit, there is a distinct jump in the values of parameter. The gray, silty-clay horizon that marks the catastrophic drainage of Glacial Lake Fraser (11,200 yr BP) is also characterized by an abrupt decrease in the value of  $b^*$  (6%).

### 5.3. $b^*$ variability

Three phases of variability can be recognized in the laboratory-determined  $b^*$  values. In the upper part of the record, from 0 to 6000 yr BP, the  $b^*$  curve shows relatively high reflectance values, but the signal is highly variable (Figs. 5 and 6). In addition, there are some very short periods with low variability. From 4600 to 7000 yr BP, the variability steadily decreases, becoming very small. The  $b^*$  values recorded for the lowermost part of the core (7000 to 11,000 yr BP) are lower and less variable than the values for the upper part (Figs. 5 and 6). The only significant variability is due to the Mazama ash and Fraser River Valley drainage deposit.

### 5.4. First derivative investigations

Variations in sediment composition were investigated downcore through the study of first derivative spectra

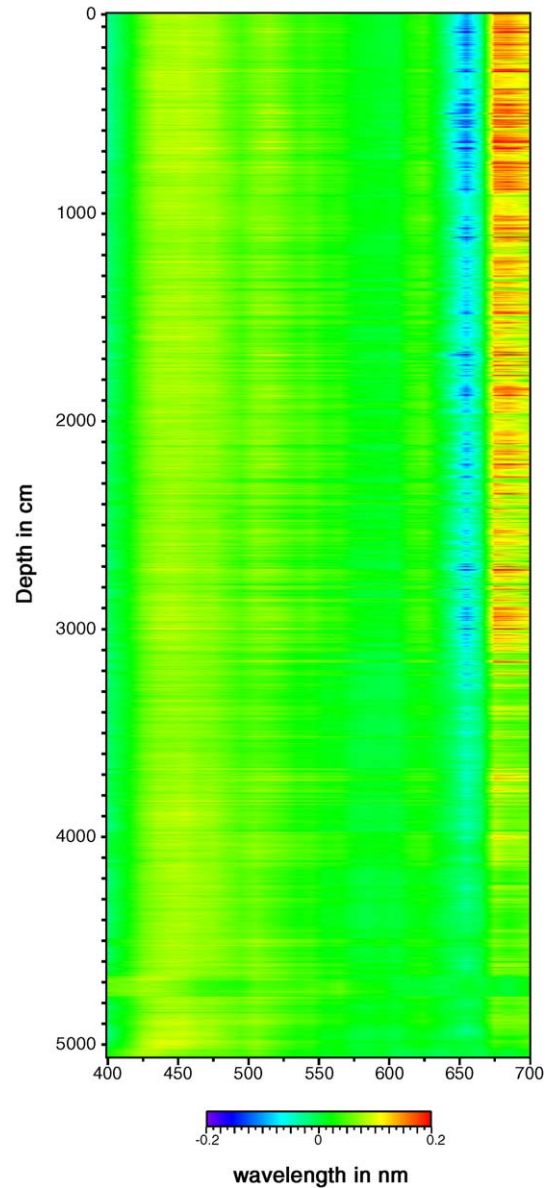


Fig. 7. Downcore changes of first derivative values. The first derivative of all 5100 spectra has been calculated and plotted on this 3D diagram. The  $X$  axis represents the wavelengths,  $Y$  is depth in core and  $Z$  the derivative value for the corresponding wavelength expressed by a code of color. The higher the first derivative the more the color tends towards the red; the lower its value the more it tends towards blue. The onset of anoxia is marked by increasing of the 675 nm first derivative value which can be related to organic content. (For interpretation of the references to colour in this figure legend, the reader is referred to the web of this article.)



(Fig. 7). A peak at 675 nm progressively emerges at 3350 cm (i.e. 7000 yr BP), concomitant with the increase in  $b^*$  signal variability. This peak remains distinct up to the present-day and exhibits the same variation and the same three-part division as the  $b^*$  signals. Furthermore, the first derivative signal at 675 nm shows the same cyclicity and the same progressive increase around 7000 yr BP as the  $b^*$  signal.

## 6. Discussion

### 6.1. Basin status change highlighted by spectrophotometry

#### 6.1.1. Differences between shipboard and land-based data

The differences in color between shipboard and laboratory-based measurements on core MD02-2490 were clearly visible. The significant changes in sediment color, as reflected in the  $b^*$  values, were mainly caused by changes in sample water content and oxidation.

Changes in water content affect several parameters (Balsam et al., 1998), including the degree of darkening which increases with increasing water content. In silt-grade and finer sediments, high water contents can disrupt the packing, making the sediment appear even darker. Thus, the increase in variability between 4000 yr BP and the present can be directly related to the water content of the sediment: sediments close to the surface are less compact and therefore have higher water contents than more deeply buried sediments. Balsam et al. (1998) suggest that color measurements should be taken on sediment that is as dry as possible and suggest 20 h to measure color. However, oxidation seems to have a greater effect on the spectra emitted by the sediment than water. One common sediment component that oxidizes is organic matter. Unoxidized organic matter is dark, and as it oxidizes, the sediment that contains it becomes lighter, usually changing from dark to light gray (Deaton and Balsam, 1993). This color change may also result from the oxidation of reduced iron compounds to iron oxides and oxyhydroxides.

The oxidation of iron compounds has the potential to lighten sediment and to increase reflectance at the red end of the spectrum. Balsam et al. (1997) showed that organic matter is one of the most commonly oxidized components and that it becomes darker with time. Conversely, non-organic sediments become clearer, usually changing from dark to light gray (Deaton and Balsam, 1993). Saanich Inlet sediments have particularly high OM contents (T.O.C.  $\approx$  2.5% to 4.5%). The progressive increase in  $b^*$  values around 7000 yr BP seems to be the

result of OM and perhaps iron monosulfide oxidation both reflecting a change in the composition of the sediment. The gradual increase in  $b^*$  from 7000 to 6000 yr BP indicates a gradual decrease in oxygen, which is compatible with the visual, sedimentological observations made by Blais-Stevens et al. (2001).

These results suggest that it may be possible to obtain more information about the mineralogy and composition of sediments using the first derivative of the spectra obtained from dry samples. Because of the effects of oxidation and changes in water content, Balsam et al. (1997) recommended not taking spectrophotometry measurements until after the preliminary measurements had been completed. Such a precaution is particularly necessary in the study of anoxic environments, where sediment color is related to the degree of oxidation (OM, Iron monosulfide).

#### 6.1.2. $b^*$ variability

As previously stated, between 4000 yr BP and the present-day, the strong variability of  $b^*$  measurements taken onboard the *Marion Dufresne* is due to variations in water content. As the samples used for the land-based measurements had been in storage for a year, their water contents had reduced and the OM had oxidized.

Differences in laboratory-determined  $b^*$  values are related to changing conditions in the basin. In anoxic environments, the lack of oxygen prevents the development of a benthic fauna, so the sediment is not bioturbated and laminations remain distinct. The reflectance measured at each point will depend on whether the instrument's 8 mm aperture alights upon a light lamina, a dark lamina, or an area including both types of laminae. Therefore, both lamina thickness, which is related to sedimentation rate, and lamina sharpness influence the signal that is measured. For well-laminated sediments, the difference between the light- and dark-colored laminae determines the maximum amplitude of the reflectance values. In oxygenated and bioturbated environments, the sediment is mixed, laminae are fewer or not visible and reflectance measurements give average values. This means that the gradual transition, at about 7000 yr BP, corresponds to a change from bioturbated (non-laminated) to non-bioturbated (laminated) conditions (Fig. 5). During periods in which anoxic conditions prevail, the short sections of sediment that show low variability may be due to either seismic events causing gravity reworking of the sediment or short-lived oxygenated conditions.

Although most of the bioturbated portion of the core shows little variability, there are two exceptions. One is the Mazama ash at 7645 yr BP: its white color affects the reflectance values of nearby sediments (Fig. 5). The

other is the Fraser River Valley drainage deposit at around 11,200 yr BP (Fig. 5). This horizon is marked by a slight increase in the variability of the signal and sedimentological descriptions note the presence of quite distinct laminae, as recorded by Blais-Stevens et al. (2003). These minor exceptions are probably due to differences in sedimentation rate and/or changes in sediment supply. They are much less distinct than the major change around 7000 yr BP, which reflects a change from oxic to anoxic conditions in the southern part of the basin (Fig. 5). Indeed anoxic conditions occurred in the southern (deeper) part of the fjord (ca. 7000 yr ago ODP 1033) earlier than in the northern part of the basin (ca. 4600 yr ago; ODP 1034). A transitional zone of oxic and anoxic conditions exists between 7000 to 4600 yr ago.

### 6.1.3. "Derived 675" as a proxy for organic matter content

According to Balsam and Beeson (2003), peaks in the first derivative at 675 nm can be interpreted as indicating the presence of organic matter (Figs. 7 and 8). In order to confirm this assumption, we made a test with sediment which shows the OM signal: we used H<sub>2</sub>O<sub>2</sub> to

remove OM and we measured color. The spectra is flat and do not highlight OM peak any more but shows a signal of clay that our spectrophotometer does not allowed to see (Fig. 8). Indeed clay signal appears between 200 and 400 nm. First derivative values at 675 nm highlights OM variation.

Variations in the OM signal can be followed downcore in Fig. 7. From Fig. 7, it is clear that a boundary exists at a depth of 3341 cm. This boundary corresponds to the onset of anoxic conditions and to the appearance of laminations. Our spectrophotometry analysis shows that the development of anoxic conditions in Saanich Inlet was accompanied by an increase in the OM content of the sediment, as widely described in the literature (e.g. McQuoid et al., 2001; Whiticar and Elvert, 2001). Several hypotheses have been proposed to explain this pattern. For example, McQuoid et al. (2001) suggest that changes in the OM content of the sediment may originate in three ways: change of the OM source — primarily marine vs. terrestrial, increased OM preservation, or changes in basin primary productivity. Both McQuoid et al. (2001) and Whiticar and Elvert (2001) suggest that variations in OM content are most likely to be caused by changes in basin primary

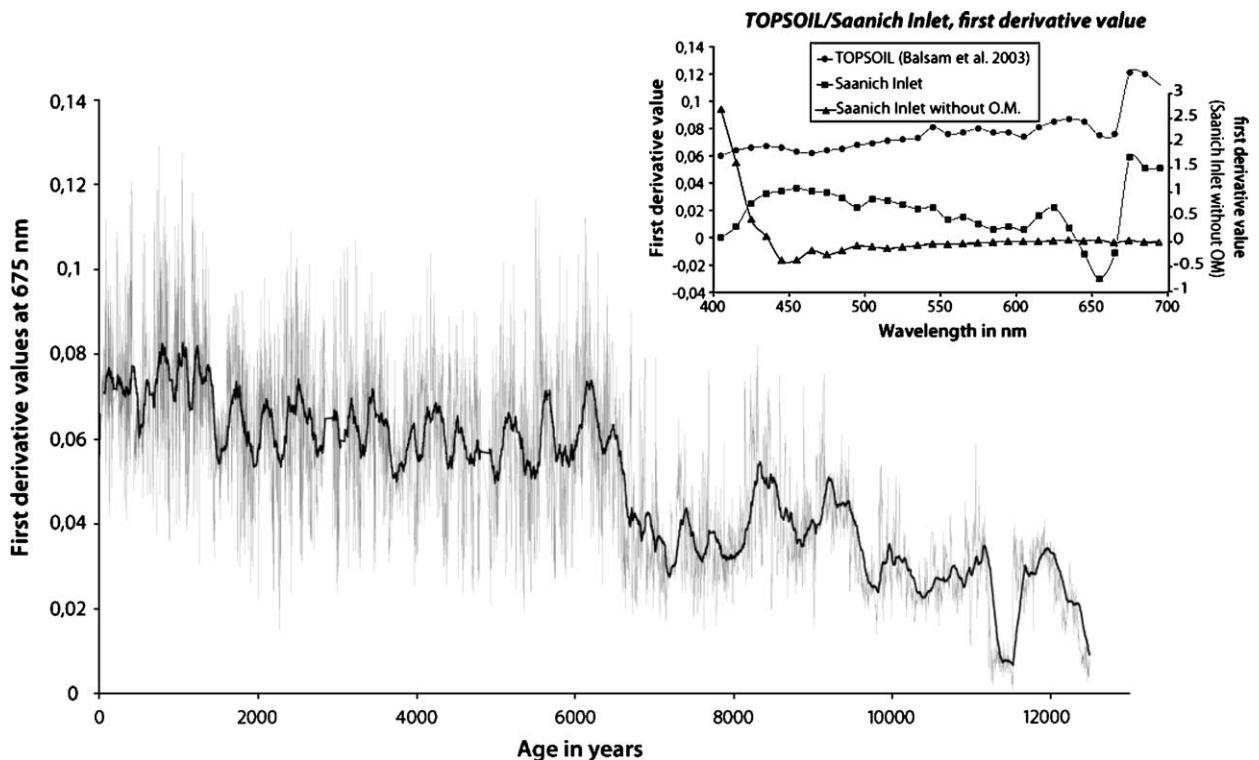


Fig. 8. Downcore variations of the 675 nm first derivative values plotted as a function of the age. The first derivative peak at 675 nm has been attributed to organic matter by Balsam and Beeson (2003).

productivity. This conclusion is supported by the fact that there is no significant change in the C:N profile during the Holocene and  $\delta^{13}\text{C}_{\text{org}}$  values become  $^{12}\text{C}$ -enriched towards the present rather than  $^{13}\text{C}$ -enriched, as would be expected if this were due to diagenesis (McQuoid et al., 2001).

### 6.2. $b^*$ as a proxy for diatom vs. detrital content

Our study suggests that the first derivative at 675 nm can be considered as proxy for OM content (Fig. 8) and that  $b^*$  can be considered as proxy for diatom content (Fig. 6). The correlation between these two parameters yields a high value ( $r=0.9$ ), suggesting a link between organic matter and diatom contents. This strong correlation is confirmed by the composition of the laminae: dark laminae have high detrital contents, whereas the lighter-colored, yellowish laminae have high diatom contents: the yellow color is not due to the opaline silica of the diatoms, it is produced by the mixture of diatoms and OM. Under an optical microscope, sediment smears from these laminae show large quantities of biogenic silica and clusters of organic matter, and it is this OM that gives the sediment its yellow/brown color. The connection between diatoms and organic matter is not surprising; Nelson et al. (1995) estimated that diatoms are responsible for 75% of the primary productivity in nutrient-rich waters, and Timothy et al. (2003) estimated that between 54% and 72% of the total organic carbon deposited in Saanich Inlet in the spring and summer is marine organic carbon produced, mostly, by diatoms. During fall and winter, this percentage decreases to 36–54%, which is in accordance with the compositional variations observed by Dean et al. (2001). With the study of 82 samples of laminated diatomaceous sediment, Johnson and Grimm (2001) have shown a close correlation between opal (varying between 14.5% and 44.9%) and organic contents (1.1% and 2.4%). According to these authors, C/N ratios and  $\delta^{13}\text{C}$  values indicate a predominant marine source (diatom-derived) of OM without a significant input of terrestrial OM. In this study, mechanism here evoked implies a high primary productivity leading, for a large part of this OM, to escape from being consumed by micro-organisms, and hence leading to their preservation in sediments.

Hence and as supported by all these previous observations, we conclude that both the first derivative and  $b^*$  indicate the presence of OM and diatoms in the anoxic upper section of the core. These two proxies can be extended to the lower section of the core even though the sediment has been subject to bioturbation.

### 6.3. Origin of cycles: high-resolution reconstruction of ocean upwelling

#### 6.3.1. A proxy for upwelling

Because diatoms are very sensitive to increased nutrient supply in the basin,  $b^*$  can be considered a proxy for biogenic silica in sediments. In Saanich Inlet, the seasonal supply of nutrients is mainly governed by frequent coastal upwelling. Upwelling conditions are common in the study area, especially from April to September when the region is under the influence of the North Pacific High. The prevailing winds generate a southward coastal drift and offshore Ekman transport, which trigger coastal upwelling (Gargett et al., 2003). Nutrients from upwelling contribute significantly to the nutrient budget along the coast of British Columbia. Therefore, variations in the supply of nutrients, if they are recorded in the sediment, provide an excellent proxy for reconstructing oceanic and atmospheric activity. Consequently,  $b^*$  can be considered a proxy for coastal upwelling and, indirectly, for the intensity of the Aleutian Depression, which exerts a strong influence on upwelling.

#### 6.3.2. $b^*$ cyclicity, upwelling intensity and sea level

As described above, the  $b^*$  values reveal three distinct stages in the evolution of the basin (Fig. 6):

1. An oxygenated stage, from ~11,000 to ~7000 yr BP, in which four cycles are present, although the last cycle is truncated. This stage is characterized by a ~150 m decrease in eustatic level as the result of the isostatic rebound following the melting of the Cordilleran ice sheet in the Coast Mountains. By 10,000 to 8000 yr BP, sea level had fallen and restricted the entry of water into the inlet through the narrow Satellite Channel (Huntley et al., 2001). The eustatic level reached its lowest point at around 8000 yr BP when isostatic rebound overcame the effects of the Holocene marine transgression (Huntley et al., 2001). This had a significant effect on the pattern of nutrient supply and consequently on the OM content of the sediment. The shallowness of the water column in the Juan Fuca Strait, and of the sill at the mouth of Saanich Inlet, prevent nutrients flowing into the inlet. Thus, during periods of low amplitude upwelling it can be argued that OM will consist of a mixture of terrestrial and oceanic input and that biogenic silica sedimentation will be closely controlled by restrictions on the amount of nutrients supplied by coastal

upwelling. Later, (around 8000 yr BP), sea level began rising steadily to reach its present level around 4000 yr BP (Clague et al., 1982; Huntley et al., 2001).

2. A transitional stage, characterized by an abrupt increase in  $b^*$  values. Around 7000 yr BP, southern part of Saanich Inlet became anoxic, due to an increase in primary productivity (see Section 6.1.3). Müller and Suess (1979) and Sancetta and Calvert (1988) suggest that this increase was probably due to bathymetric changes south of Vancouver Island that restricted the circulation of water causing an increase in eutrophication and in the accumulation and burial of organic matter. However, during the 2000–3000 yr interval before the establishment of anoxic conditions, the circulation of water in Saanich Inlet was more restricted than it is at present, and the basin remained oxygenated. Furthermore, the inlet had similar bathymetry 10,000 yr BP as it did 4000 yr BP (Huntley et al., 2001). Hence, restricted water circulation cannot be the factor that determines the development of anoxic conditions in Saanich Inlet. We suggest that water charged with nutrients was supplied by upwelling in the Juan de Fuca Strait, but this water could not enter Saanich Inlet until a particular water depth was reached. Anoxic conditions could only form in the basin when the sill was deep enough to allow upwelling nutrient-charged water to cross the sill. The difference between the beginning of anoxia in the southern and northern part of the inlet comes from a difference of bathymetry. Indeed, MD02-2490 being the deepest record becomes anoxic in first.
3. An anoxic stage, from 7000 yr BP to the present (4600 yr cal BP in the northern part), which shows strong cyclicity. This cycle exists because sea level is sufficiently high for most of the upwelling water to cross the sill and deliver its nutrients to the fjord. (Fig. 7). Dean and Kemp (2004) applied high-resolution scanning electron microscopy and time series analysis techniques to Saanich Inlet varved-sediments. For a small portion of sediment dated at around 2100 yr BP, they identified sub-decadal periods linked to the Quasi-Biennial Oscillation (QBO) and the El Niño Southern Oscillation (ENSO), and decadal periods linked to the Pacific Decadal Oscillation (PDO). We can hypothesize that our study provides a multi-decadal high frequency signal analysis on a very short time scale that cannot be extendable after 4600 yr BP because of the gradual appearance of anoxic conditions; however, it shows the main factors

controlling the laminated deposits. From the study of Holocene sediment color, we can infer that the same phenomena occurred at a lower frequency on a centennial scale (Nederbragt and Thurow, 2005). Our work has shown variations in nutrient and OM supply (terrestrial vs. diatom end-members) to Saanich Inlet. It seems likely that these variations were influenced by the QBO, ENSO and PDO throughout the Holocene. However, the relative effects of each of these three atmospheric phenomena remain unclear.

## 7. Conclusions

The comparison between shipboard and laboratory spectrophotometry data confirms the assertion made by Chapman and Shackleton (1998) and by Balsam et al. (1999) that water content may adversely affect spectral measurements. Furthermore, to extract the greatest possible amount of information from a core sample, the sample must be allowed to oxidize. The time required for the oxidation process needs to be carefully determined.

Analysis of core MD02-2490 shows that reflectance spectrophotometry, which allows the rapid acquisition of data without damaging the core, is a useful tool for identifying variations in sediment components. These variations can be interpreted in terms of changes in paleoceanic conditions. In Saanich Inlet, these changes were examined on a centennial scale using the  $b^*$  parameter and the first derivative of specific spectral wavelengths. The validity of the method was demonstrated by its ability to identify the well-known transition between the two basin states that occurred around 7000 yr BP in the southern part and the two well-documented stratigraphic markers.

The  $b^*$  parameter provides a proxy for diatom vs. detrital input and the first derivative spectral value at 675 nm indicates OM content. The close correlation between these two proxies suggests that a significant proportion of the organic matter is produced by diatoms.

The high-resolution reconstruction of upwelling intensity shows that the relationship between changes in sea level and the depth of the sill at the mouth of the inlet plays a key role in basin sedimentation. This reconstruction is based on downcore variations in OM. Although this OM is mostly derived from diatoms, there was significant terrestrial OM input during the Late Holocene. The OM content of the sediment is sensitive to fluctuations in nutrient supply to the inlet induced by increases in upwelling intensity.



## Acknowledgements

Core MD02-2490 was retrieved during the IMAGES VIII MONA Cruise of the *RV Marion Dufresne*. The ship and the scientific instruments were provided by the Paul-Emile Victor Polar Institute (IPEV). The scientific program was strongly supported by a team from the IPEV under the direction of Yvon Balut. We would also like to thank Guillaume Saint-Onge for his help on the ship. Murray Hay, Jérôme Nomade, Taoufik Radi, Anne deVernal and Frank Whitney provided constructive and valuable comments. Our sincere thanks to all of them. The Minolta CM 2600-d was financed by the French Mountain Institute.

We wish to thank David J.W. Piper for constructive observations and comments. We also acknowledge Andr e Blais-Stevens and John Clague for their detailed review.

## References

- Bacon, C.R., 1983. Eruptive history of Mt Mazama and Crater Lake Caldera, Cascade range, USA. *J. Volcanol. Geotherm. Res.* 18, 57–115.
- Balsam, W.L., Beeson, J.P., 2003. Sea-floor sediment distribution in the Gulf of Mexico. *Deep-Sea Res., Part 1, Oceanogr. Res. Pap.* 12, 1421–1444.
- Balsam, W.L., Deaton, B.C., 1991. Sediment dispersal in the Atlantic Ocean: evaluation by visible light spectra. *Rev. Aquat. Sci.* 4, 411–447.
- Balsam, W.L., Deaton, B.C., 1996. Determining the composition of Late Quaternary marine sediments from NUV, VIS, and NIR diffuse reflectance spectra. *Mar. Geol.* 134 (1–2), 31–55.
- Balsam, W.L., Damuth, J.E., Schneider, R.R., 1997. Comparison of shipboard vs shore-based spectral data from Amazon Fan cores: implications for interpreting sediment composition. *Ocean Drill. Program Sci.* 155s, 193–215.
- Balsam, W.L., Deaton, B.C., Damuth, J.E., 1998. The effects of water content on diffuse reflectance spectrophotometry studies of deep-sea sediment cores. *Mar. Geol.* 149 (1–4), 177–189.
- Balsam, W.L., Deaton, B.C., Damuth, J.E., 1999. Evaluating optical lightness as a proxy for carbonate content in marine sediment cores. *Mar. Geol.* 161 (2–4), 141–153.
- Barranco Jr., F.T., Balsam, W.L., Deaton, B.C., 1989. Quantitative reassessment of brick red lutites: evidence from reflectance spectrophotometry. *Mar. Geol.* 89 (3–4), 299–314.
- Blais, A., 1995. Foraminiferal biofacies and Holocene sediments from Saanich Inlet, British Columbia: implications for environmental and neotectonic research [Ph.D. thesis]. Carleton University, Ottawa, ON, Canada.
- Blais-Stevens, A., Bornhold, B.D., 1998. Holocene spring flood deposits in Saanich Inlet, B.C.: a paleoclimatic record? Geological Association of Canada Annual Meeting. May 18–20, 1998, Qu bec, Qu bec, Canada, p. A-20. Abstract Volume.
- Blais-Stevens, A., Clague, J.J., 2001. Paleoseismic signature in late Holocene sediment cores from Saanich Inlet, British Columbia. *Mar. Geol.* 175 (1–4), 131–148.
- Blais-Stevens, A., Bornhold, B.D., Kemp, A.E.S., Dean, J.M., Vaan, A.A., 2001. Overview of Late Quaternary stratigraphy in Saanich Inlet, British Columbia: results of Ocean Drilling Program Leg 169S. *Mar. Geol.* 174 (1–4), 3–20 (15 March).
- Blais-Stevens, A., Clague, J.J., Mathewes, R.W., Hebda, R.J., Bornhold, B.D., 2003. Record of large, Late Pleistocene outburst floods preserved in Saanich Inlet sediments, Vancouver Island, Canada. *Quat. Sci. Rev.* 22 (21–22), 2327–2334.
- Bobrowsky, P.T., Clague, J.J., 1990. Holocene sediments from Saanich Inlet, British Columbia, and their neotectonic implications. *Pap. [0151] Geol. Surv. Can.*, vol. 90-1E, pp. 251–256.
- Bornhold, B.D., Firth, J., Leg 169s shipboard scientific party, 1996. Ocean Drilling Program Leg 169s Scientific Prospectus Saanich Inlet. Scientific Prospectus No. 69S.
- Calvert, S.E., Pedersen, T.F., Karlin, R.E., 2001. Geochemical and isotopic evidence for post-glacial palaeoceanographic changes in Saanich Inlet, British Columbia. *Mar. Geol.* 174 (1–4), 287–305.
- Carter, N.M., 1934. Physiography and oceanography of some British Columbia fjords. *Proceedings in of the Fifth Pacific Science Congress, 1933*, vol. 1. Pacific Science Association, Vancouver, BC, pp. 721–733.
- Chapman, M.R., Shackleton, J., 1998. What level of resolution is attainable in a deep-sea core? Results of a spectrophotometer study. *Paleoceanography* 13 (4), 311–315.
- Clague, J.J., Harper, J.R., Hebda, R.J., Howes, D.E., 1982. Late Quaternary sea levels and crustal movements, coastal British Columbia. *Can. J. Earth Sci.* 19, 597–618.
- Clague, J.J., James, T.S., 2002. History and isostatic effects of the last ice sheet in southern British Columbia. *Quat. Sci. Rev.* 21 (1–3), 71–87.
- Cowan, E.A., 2001. Late Pleistocene glacial marine record in Saanich Inlet, British Columbia. *Mar. Geol.* 174 (1–4), 43–57.
- Dean, J.M., Kemp, A.E.S., 2004. A 2100 year BP record of the Pacific Decadal Oscillation, El Ni o Southern Oscillation and Quasi-Biennial Oscillation in marine production and fluvial input from Saanich Inlet, British Columbia. *Palaeogeogr. Palaeoclimatol. Palaeoecol.* 213, 207–229.
- Dean, J.M., Kemp, A.E.S., Pearce, R.B., 2001. Palaeo-flux records from electron microscope studies of Holocene laminated sediments, Saanich Inlet, British Columbia. *Mar. Geol.* 174 (1–4), 139–158.
- Deaton, B.C., Balsam, W.L., 1991. Visible spectroscopy—a rapid method for determining hematite and goethite concentration in geological materials. *J. Sediment. Petrol.* 61, 628–632.
- Deaton, B.C., Balsam, W.L., 1993. Identifying production zones with NUV/VIS/NIR spectra: examples from the Caddo Limestone and Strawn Sand. *Geol. Soc. Am., Abstr. Programs*, vol. 25, p. 8.
- Gargett, A.E., Stucchi, D., Whitney, F., 2003. Physical processes associated with high primary production in Saanich Inlet, British Columbia. *Estuar. Coast. Shelf Sci.* 56, 1141–1156.
- Gross, M.G., Gucluer, S.M., Creager, J.S., Dawson, W.A., 1963. Varved marine sediments in a stagnant fjord. *Science* 141, 918–919.
- Helmke, J.P., Schultz, M., Bauch, H.A., 2002. Sediment-color record from the northeast Atlantic reveals patterns of millennial-scale climate variability during the past 500,000 yrs. *Quat. Res.* 57, 49–57.
- Herbert, T.D., Tom, B.A., Burnett, C., 1992. Precise major component determinations in deep-sea sediments using Fournier transform infrared spectroscopy. *Geochim. Cosmochim. Acta* 56, 1759–1763.
- Herlinveau, R.H., 1962. Oceanography of Saanich Inlet in Vancouver Island, British Columbia. *J. Fish. Res. Board Can.* 19, 1–37.



- Hutchinson, I., James, T.S., Reimer, P.J., Bornhold, B.D., Clague, J.J., 2004. Marine and limnic radiocarbon reservoir corrections for studies of late- and postglacial environments in Georgia Basin and Puget Lowland, British Columbia, Canada and Washington, USA. *Quat. Res.* 61 (2), 193–203.
- Huntley, D.H., Bobrowsky, P.T., Clague, J.J., 2001. Ocean drilling program Leg 169S: surficial geology, stratigraphy and geomorphology of the Saanich Inlet area, southeastern Vancouver Island, British Columbia. *Mar. Geol.* 174 (1–4), 27–41.
- Johnson, K.M., Grimm, K.A., 2001. Opal and organic carbon in laminated diatomaceous sediments: Saanich Inlet, Santa Barbara Basin and the Miocene Monterey Formation. *Mar. Geol.* 174 (1–4), 159–175 (15 March).
- McQuoid, M.R., Hobson, L.A., 2001. A Holocene record of diatom and silicoflagellate microfossils in sediments of Saanich Inlet, ODP Leg 169S. *Mar. Geol.* 174 (1–4), 111–123.
- McQuoid, M.R., Whiticar, M.J., Calvert, S.E., Pedersen, T.F., 2001. A post-glacial isotope record of primary production and accumulation in the organic sediments of Saanich Inlet, ODP Leg 169S. *Mar. Geol.* 174 (1–4), 273–286.
- Mix, A.C., Rugh, W., Pisias, N.G., Veirs, S., Leg 138 Shipboard Sedimentologists (Hagelberg, T., Hovan, S., Kemp, A., Leinen, M., Levitan, M., Ravelo, C.), Leg 138 Scientific Party, 1992. Color reflectance spectroscopy: a tool for rapid characterization of deep-sea sediments. In: Mayer, L., Pisias, N., Janecek, T., et al. (Eds.), *Proc. ODP, Init. Repts.*, vol. 138 (Pt. 1). Ocean Drilling Program, College Station, TX, pp. 66–67.
- Mosher, D.C., Moran, K., 2001. Post-glacial evolution of Saanich Inlet, British Columbia: results of physical property and seismic reflection stratigraphic analysis. *Mar. Geol.* 174 (1–4), 59–77.
- Müller, P.J., Suess, E., 1979. Productivity, sedimentation rate and sedimentary organic matter in oceans. I. Organic matter preservation. *Deep-Sea Res.* 26, 1347–1362.
- Nederbragt, A.J., Thurow, J.W., 2001. A 6000 yr varve record of Holocene climate in Saanich Inlet, British Columbia, from digital sediment colour analysis of ODP Leg 169S cores. *Mar. Geol.* 174 (1–4), 95–110.
- Nederbragt, A.J., Thurow, J.W., 2005. Geographic coherence of millennial-scale climate cycles during the Holocene. *Palaeogeogr. Palaeoclimatol. Palaeoecol.* 221, 313–324.
- Nelson, D.M., Tréguer, P., Brzezinski, M.A., Leynaert, A., Quéguiner, B., 1995. Production and dissolution of biogenic silica in the ocean: revised global estimates, comparisons with regional data and relationship to biogenic sedimentation. *Glob. Biogeochem. Cycles* 9 (3), 359–372.
- O’Connell, J.M., Tunnicliffe, V., 2001. The use of sedimentary fish remains for interpretation of long-term fish population fluctuations. *Mar. Geol.* 174 (1–4), 177–195.
- Pellatt, M.G., Hebda, R.J., Mathewes, R.W., 2001. High-resolution Holocene vegetation history and climate from Hole 1034B, ODP leg 169S, Saanich Inlet, Canada. *Mar. Geol.* 174 (1–4), 211–222.
- Robinson, S.W., Thompson, G., 1981. Radiocarbon corrections for marine Shell dates with application to southern Pacific Northwest Coast prehistory. *Syesis* 14, 45–57.
- Sancetta, C., Calvert, S.E., 1988. The annual cycle of sedimentation in Saanich Inlet, British Columbia: implications for the interpretation of diatom fossil assemblages. *Deep-sea Res.* 35, 71–90.
- Schneider, R.R., Cramp, A., Damuth, J.E., Hiscott, R.N., Kowsmann, R.O., Lopez, M., Nanayama, F., Normark, W.R., Shipboard Scientific Party, 1995. Color-reflectance measurements obtained from leg 155 cores. In: Flood, R.D., Piper, D.J.W., Klaus, A., et al. (Eds.), *Proc. ODP, Init. Repts.*, vol. 155. Ocean Drilling Program, College Station, TX, pp. 1–65.
- Timothy, D.A., Soon, M.Y.S., Calvert, S.E., 2003. Settling fluxes in Saanich and Jervis Inlets, British Columbia, Canada: sources and seasonal patterns. *Prog. Oceanogr.* 59 (1), 31–73.
- Tunnicliffe, V., O’Connell, J.M., McQuoid, M.R., 2001. A Holocene record of marine fish remains from the Northeastern Pacific. *Mar. Geol.* 174 (1–4), 197–210.
- Whiticar, M.J., Elvert, M.E., 2001. Organic geochemistry of Saanich Inlet, BC, during the Holocene as revealed by Ocean Drilling Program Leg 169S. *Mar. Geol.* 174 (1–4), 249–271.